

User Access Mode Selection in Fog Computing Based Radio Access Networks

Shi Yan, Mugen Peng, *Senior Member, IEEE*, and Wenbo Wang *Member, IEEE*.
Key Laboratory of Universal Wireless Communication, Ministry of Education
Beijing University of Posts and Telecommunications, Beijing, 100876, China

Abstract—Fog computing based radio access network is a promising paradigm for the fifth generation wireless communication system to provide high spectral and energy efficiency. With the help of the new designed fog computing based access points (F-APs), the user-centric objectives can be achieved through the adaptive technique and will relieve the load of fronthaul and alleviate the burden of base band unit pool. In this paper, we derive the coverage probability and ergodic rate for both F-AP users and device-to-device users by taking into account the different nodes locations, cache sizes as well as user access modes. Particularly, the stochastic geometry tool is used to derive expressions for above performance metrics. Simulation results validate the accuracy of our analysis and we obtain interesting tradeoffs that depend on the effect of the cache size, user node density, and the quality of service constrains on the different performance metrics.

I. INTRODUCTION

The fifth generation (5G) mobile wireless system is proposed to be initially deployed in 2020. Compared with the current fourth generation (4G) mobile wireless system, it is given the envision of 1000 times higher wireless area capacity and is expected to save up to 90% of energy consumption per service compared with the current fourth generation (4G) mobile wireless system [1]. To achieve these goals and alleviate the existing challenges in cloud radio access networks (C-RANs) [2] [3], the fog computing radio access network (F-RAN) has been proposed as a new network architecture by incorporating of fog computing, edge storage and centralized cloud computing into radio access networks [4].

Fog computing, which is similar to edge computing, is first proposed by Cisco [5]. It extends cloud computing and services to the edge of the network. In F-RANs, services cannot only be executed in a centralized unit such as the BBU pool in C-RAN, but also can be hosted at smart terminal devices which are closer to the users. Meanwhile, through the user-centric adaptive techniques such as device-to-device (D2D), distributed coordination, and large-scale centralized cooperation, users don't have to connect to the centralized cloud computing unit to complete the data transmission, which will relieve the load of fronthaul and alleviate the burden of BBU pool. In order to execute the above, the traditional access point (AP) is evolved to the fog computing based access point (F-AP) through equipped with a certain caching and sufficient computing capabilities to execute the local cooperative signal processing in the physical layer.

Many previous works have been done to analyze the ergodic rate performance of C-RAN systems. In [6], the ergodic rate

of distributed remote radio heads (RRHs) is characterized in C-RAN with spatially single antenna random locations and the minimum number of RRHs for the desired user to meet a predefined quality of service is analyzed. In [7], it is demonstrated that the large scale fading exponent has a significant impact on the capacity of large C-RAN systems.

However, the fronthaul limitation between RRHs and Cloud is a remarkable challenge to block the commercial practices. Consequently, taking advantage of the fog-computing to switch the content cache or data process to users is the key to improve both spectrum and energy efficiency as well as can relieve the load of fronthaul in cloud computing based network architectures. D2D communications as an adaptive technology not only can provide the efficient utilization of available radio resources to improve the connectivity of devices, but also has the ability of supporting proximity-based services, such as social networking applications and content sharing. Existing research on D2D networks is mainly focused on underlaid cellular networks with fixed location model [8] ~ [10]. Different from the traditional underlaid cellular networks, the main challenge to analyze the rate performance in F-RAN is that the F-APs are often deployed randomly and the severe intra-tier and inter-tier interference may drastically deteriorate the performance of both the D2D and F-AP users.

In this paper, we analyze the coverage probability and ergodic rate with three user access modes in a downlink F-RAN, where both the F-AP nodes and D2D users are modeled as spatial Poisson Point Process (PPP) distribution. The contributions are three-folds.

- The ergodic rates of D2D mode, nearest F-AP mode, local distributed coordination mode, and coverage probability of the first two modes in F-RAN system are characterized, where both the intra-tier and inter-tier interference and distributed cache are considered.
- The closed-form expressions for the ergodic rate are presented in some special cases, which can make the analysis not only tractable, but also flexible. Moreover, based on the proposed performance metrics, the impacts of the cache size, user node density, and the quality of service (QoS) constrains are characterized.
- The Monte Carlo simulation results evaluate impacts of the F-AP nodes density, SIR threshold, cache size and association schemes on the ergodic rate. And an adaptation user access mode selection mechanism is proposed to improve F-RAN system performances.

II. SYSTEM MODEL

A. F-RAN System Model

A F-RAN downlink system is considered in this paper, where a group of F-APs are deployed according to a two-dimensional PPP Φ_f with density of λ_f in a disc plane \mathcal{D}^2 . As the new designed AP, F-AP integrates not only the front radio frequency (RF) but also the physical processing functionalities and procedures of the upper layers, which made F-AP has a sufficient computing capabilities to execute the local cooperative signal processing in the physical layer and implement the caching resource management.

We assume the spatial distribution of users is modeled as an independent PPP Φ_u distribution with constant intensity λ_u . By setting $p \sim (0, 1]$ as the probability that a user support direct connection to other intelligent terminal users, i.e., D2D, the distribution of the D2D users location can be denoted as a thinning homogeneous Φ_{du} with the density of $\lambda_{du} = p\lambda_u$. Meanwhile according to Marking Theorem, the distribution of F-AP users follows a stationary PPP Φ_{fu} with the density of $\lambda_{fu} = (1 - p)\lambda_u$. Without any loss of generality, each F-AP and D2D user is assumed as single antenna configuration with a fixed transmission power, defined as P_f and P_d , respectively, and our analysis is focus on a desired user (denoted by U) located at the origin of the disc \mathcal{D}^2 .

B. Cache Model

In this paper, we consider there are N video contents in the network, and all the video contents are assumed to have the same distribution. Each of the D2D user and F-AP has a limited caching storage space with the size of C_d and C_f , respectively, and $C_d < C_f < N$.

In previous research, it has been found that people are always interested in the most popular video contents [11]. In other word, only a small portion of the N contents are frequently accessed by the majority of users. Therefore, the demand probability of the i -th popularity video content can be modeled as the following Zipf distribution

$$f_i(\sigma, N) = \frac{1/i^\sigma}{\sum_{k=1}^N 1/k^\sigma}, \quad (1)$$

where the video content with a smaller index has a larger probability of being requested by users, i.e. $f_i(\sigma, N) > f_j(\sigma, N)$, if $i < j$. Zipf exponent $\sigma > 0$ controls the relative popularity of files, and with the larger σ the caching storage has a fewer of popular video contents accounting for the majority of the requests.

Content caching probability is defined as the probability of an event that the desired user U can find it requested video content V in its corresponding caching, i.e., $p_c^x = \Pr(V \in C_x)$, where x denotes the node of user accessed. By setting the caching storages in D2D users and F-APs can only cache the most popularly requested video contents, the content caching probabilities of each D2D user and F-AP can be respectively denoted as

$$p_c^D = \Pr(V \in C_d) = \sum_{i=1}^{C_d} f_i(\sigma_d, N) \quad (2)$$

$$p_c^F = \Pr(V \in C_f) = \sum_{i=1}^{C_f} f_i(\sigma_f, N). \quad (3)$$

As (2) and (3) shown, the same kind of node has the same content caching probability. In other words, each D2D user in area \mathcal{D}^2 store the same content cache, and video contene cached in different F-APs are also the same.

C. User Access Modes

In this paper, we consider users will access to the F-RAN by three user-centric access modes according to users' communication distance, content caching probability and the QoS requirements, named: D2D mode, nearest F-AP mode and local distributed coordinated mode. Let $U \rightarrow X$ signify that desired user U is associated to a node located at X , and $\|X\|$ denotes the distance between U and X .

- **D2D mode:** D2D mode is enabled when the desired user U support D2D mode and it can successfully obtain the requested contents from another D2D user in a known location within a distance threshold L_d meanwhile the signal-to-interference ratio (SIR) γ_d between the two D2D users is larger than a pre-set SIR threshold T_d . Thus,

$$\Psi_D = \{X_d : X_d \in \Phi_{du}, \|X\| \leq L_d, V \in C_d, \gamma_d \geq T_d\}. \quad (4)$$

- **Nearest F-AP mode:** When the desired user U does not support D2D mode, or U support D2D mode but the requested content V is not cached in its nearby D2D user or the SIR γ_d is not achieved the SIR threshold T_d . Thus, U try to access its nearest F-AP node which can respond to the desired user's content request, and the SIR γ_f between them is larger than SIR threshold T_f . The associated F-AP for user U can be obtained as:

$$\Psi_F = \{X_f : \arg \min_{X \in \Phi_f} (\|X\|), V \in C_f, \gamma_f \geq T_f, U \notin \Phi_{du} \cup V \notin C_d \cup \gamma_d < T_d\}. \quad (5)$$

- **Local distributed coordination mode:** The local distributed coordination mode means that the desired user U associates to multiple F-APs near to it in a user-centric cluster with a radius L_c . In this mode F-RAN can adjust the value of L_c to satisfy well with the requirement of video content and the quality of SIR.

$$\Psi_C = \{X_c : X \in \Phi_f, \forall X \in B(U, L_c) \cap \Phi_f\}, \quad (6)$$

where $B(a, b)$ denote all the point in a circle centered in a with radius b .

D. Signal-to-Interference Ratio

In this paper, we focus on the interference-limited scenario since the interference is much larger than the noise, i.e., the noise can be neglected and the SIR is dominated. Path loss is represented by $\|X\|^{-\alpha}$, where $\alpha > 2$ is the path loss exponent. We denote α_d as the path loss exponent for D2D user link and α_f as the path loss exponent for F-AP to common user or F-AP to D2D user link.

Then, if U is served by a D2D user which has a fixed distance of $\|X_d\|$ to U , the received SIR at the desired user is given by

$$SIR(U \rightarrow X_d) = \gamma_d = \frac{P_d h_d \|X_d\|^{-\alpha_d}}{I_{d,du} + I_{f,du}}, \quad (7)$$

where h_d characterize the flat Rayleigh channel fading between two D2D users, and $\|X_d\|^{-\alpha_d}$ denotes the path loss. $I_{d,du} = \sum_{i \in \Phi_{du}/d} P_d g_i r_i^{-\alpha_d}$ denotes interference from other D2D users, $g_i \sim \exp(1)$ and $r_i^{-\alpha_d}$ denote the exponentially distributed fading power over the Rayleigh fading channel and path loss from other D2D user to U , respectively. $I_{f,du} = \sum_{j \in \Phi_f} P_f g_j l_j^{-\alpha_f}$ denotes inter-tier interference from F-APs, the definition of g_j and $l_j^{-\alpha_f}$ are similar to that in $I_{d,du}$.

Next, if U is served by a single nearest F-AP in nearest F-AP mode, the SIR is given by

$$SIR(U \rightarrow X_f) = \gamma_f = \frac{P_f h_f \|X_f\|^{-\alpha_f}}{I_{f,fu} + I_{d,fu}}, \quad (8)$$

where $I_{f,fu} = \sum_{i' \in \Phi_{f/f}} P_f g_{i'} l_{i'}^{-\alpha_f}$, and $I_{d,fu} = \sum_{j' \in \Phi_{du}} P_d g_{j'} r_{j'}^{-\alpha_d}$ denote the intra-tier interference from other F-APs and inter-tier interference from D2D users, respectively.

Finally, if the local distributed coordination mode is selected, U is not only served by the single nearest F-AP, but several potential F-APs which form a F-AP cluster in (6). The F-AP cluster formation leads to that the received signal of the desired user is a sum form and after considering the inter-tier and intra-tier interference, the received SIR of U in local distributed coordination mode can be given by

$$SIR(U \rightarrow X_c) = \gamma_c = \frac{\sum_{c \in \Psi_c} P_f h_c \|X_c\|^{-\alpha_f}}{I_{f,cu} + I_{d,fu}}, \quad (9)$$

where the intra-tier interference from the F-APs out of the cluster denotes as $I_{f,cu} = \sum_{v \in \Phi_{f/\Psi_c}} P_f g_v l_v^{-\alpha_f}$, and the inter-tier interference expression $I_{d,fu}$ is equal to that in (8).

III. PERFORMANCE ANALYSIS

In this section, we derive the coverage probability and ergodic rate for F-RAN with three different association modes. The ergodic rate is defined as $R_x = p_x \mathbb{E}[\ln(1 + SIR(U \rightarrow X_x)) | SIR(U \rightarrow X_x) > T_x]$, where p_x denote the probability of the desired user U select the x mode and the unit of the ergodic rate is in terms of nats/s/Hz. $\mathbb{E}(\cdot)$ is the expectation respect to the channel fading distribution as well as the locations of the random transmitter nodes.

A. D2D mode

In D2D communications, a direct link is established between the desired user U and its service D2D user which has a known location X_d . The probability of X_d located in distance threshold L_d meanwhile has the requested content V can be given as

$$p_D = p(1 - \exp(-\pi \lambda_{du} p_c^D L_d^2)). \quad (10)$$

Proof: By using the property of 2-D Poisson process, the probability distribution of the nodes number m in a circle area πl^2 with radius limit l can be derived as

$$\Pr\{\Phi(\pi l^2) = m\} = \frac{(\lambda_X \pi l^2)^m e^{-\lambda_X \pi l^2}}{(m)!}. \quad (11)$$

Let $l = L_d$, $\lambda_X = p_c^D \lambda_{du}$ and $m = 0$. Then, we have the probability of none D2D user has the requested video content V within the distance limit L_d . Therefore, (10) can be given as the probability of complementary events and multiply the probability of U support D2D mode. ■

The probability of SIR γ_d between the two D2D users larger than a SIR threshold T_d is also called coverage probability. And in D2D mode

$$\begin{aligned} P_D(T_d, \alpha_f, \alpha_d, \|X_d\|) &= \Pr\left(\frac{P_d h_d \|X_d\|^{-\alpha_d}}{I_{d,du} + I_{f,du}} \geq T_d\right) \\ &= \Pr\left(h_d \geq \frac{T_d \|X_d\|^{\alpha_d}}{P_d} (I_{d,du} + I_{f,du})\right) \\ &\stackrel{(a)}{=} \mathbb{E}\left[\exp\left(-\frac{T_d \|X_d\|^{\alpha_d}}{P_d} (I_{d,du} + I_{f,du})\right)\right] \\ &\stackrel{(b)}{=} L_{I_{d,du}}\left(\frac{T_d \|X_d\|^{\alpha_d}}{P_d}\right) L_{I_{f,du}}\left(\frac{T_d \|X_d\|^{\alpha_d}}{P_d}\right) \\ &= \exp\left(-\pi \|X_d\|^{\frac{2\alpha_d}{\alpha_f}} \left(\lambda_{du} + \left(\frac{P_f}{P_d}\right)^{\frac{2}{\alpha_f}} \lambda_f\right) C(\alpha_f) T_d^{\frac{2}{\alpha_f}}\right), \end{aligned} \quad (12)$$

where (a) follows from the Laplace transform of $h_d \sim \exp(1)$ and the independence of $I_{d,du}$ and $I_{f,du}$ [12] [13]. (b) follows from letting $s = T_d \|X_d\|^{-\alpha_d} / P_d$ in the Laplace transforms of $I_{d,du}$ and $I_{f,du}$, $C(\alpha_f) = 2\pi \csc(2\pi/\alpha_f)/\alpha_f$.

Then, the ergodic rate for D2D mode under the conditions in (4) can be derived as

$$\begin{aligned} R_d &= p_D \mathbb{E}[\ln(1 + \gamma_d) | \gamma_d \geq T_d] \\ &\stackrel{(a)}{\approx} p_D \ln(T_d) P_D(T_d, \alpha_f, \alpha_d \|X_d\|) - \frac{p_D \alpha_f}{2} \\ &\quad \cdot \text{Ei}\left[-T_d^{\frac{2}{\alpha_f}} \pi \|X_d\|^{\frac{2\alpha_d}{\alpha_f}} \left(\lambda_{du} + \left(\frac{P_f}{P_d}\right)^{\frac{2}{\alpha_f}} \lambda_f\right) C(\alpha_f)\right], \end{aligned} \quad (13)$$

where (a) follows in the high SIR conditions $\ln(1 + \gamma_d) \rightarrow \ln(\gamma_d)$, $\text{Ei}[s] = -\int_{-\infty}^{\infty} e^{-t}/t dt$ is the exponential integral function.

Proof: See Appendix A. ■

B. Nearest F-AP mode

Next, we focus on the nearest F-AP mode which will be triggered if the desired user U cannot meet the conditions of D2D mode, i.e.,

$$p_F = 1 - p_D P_D(T_d, \alpha_f, \alpha_d, \|X_d\|). \quad (14)$$

In this mode, the desired user will try to access its nearest F-AP X_f which has the requested content V . The probability density function (PDF) of the distance between X_f and U can be derived by using a similar way as (10)

$$\begin{aligned} f_{\|X_f\|}(r_f) &= \frac{\partial(1 - \Pr(\text{No F-AP closer than } r_f))}{\partial r_f} \\ &= \frac{\partial\left(1 - \exp\left(-\pi \lambda_f p_c^F r_f^2\right)\right)}{\partial r_f} = 2\pi \lambda_f p_c^F r_f e^{-\pi \lambda_f p_c^F r_f^2}. \end{aligned} \quad (15)$$

Thus, the coverage probability of nearest F-AP mode can be calculated as

$$\begin{aligned}
P_F(T_f, \alpha_f, p_c^F) &= \Pr\left(\frac{P_f h_f \|X_f\|^{-\alpha_f}}{I_{f,fu} + I_{d,fu}} \geq T_f\right) \\
&= \int_0^\infty \Pr\left(h_f \geq \frac{T_f r_f^{\alpha_f}}{P_f} (I_{f,fu} + I_{d,fu})\right) f_{\|X_f\|}(r_f) dr_f \\
&\stackrel{(a)}{=} \int_0^\infty L_{I_{f,fu}}\left(\frac{T_f r_f^{\alpha_f}}{P_f}\right) L_{I_{d,fu}}\left(\frac{T_f r_f^{\alpha_f}}{P_f}\right) f_{\|X_f\|}(r_f) dr_f \\
&\stackrel{(b)}{=} \int_0^\infty \exp\left(-\pi \lambda_f r_f^2 p_c^F \rho(T_f, \alpha_f)\right) \\
&\cdot \exp\left(-\pi \lambda_{du} r_f^2 C(\alpha_f) \left(\frac{P_d T_f}{P_f}\right)^{\frac{2}{\alpha_f}}\right) 2\pi p_c^F \lambda_f r_f e^{-\pi p_c^F \lambda_f r_f^2} dr_f \\
&= \frac{1}{1 + \rho(T_f, \alpha_f) + \frac{\lambda_{du}}{p_c^F \lambda_f} C(\alpha_f) \left(\frac{P_d T_f}{P_f}\right)^{2/\alpha_f}}, \tag{16}
\end{aligned}$$

where (a) follows the setting of $h_f \sim \exp(1)$ and the independence between inter-floor interference $I_{d,fu}$ and intra-floor interference $I_{f,fu}$; equation (b) follows the definition of the Laplace transform, and $\rho(T_f, \alpha_f) = \int_{T_f}^{-\frac{2}{\alpha_f}} \frac{T^{2/\alpha_f}}{1+v\alpha_f/2} dv$.

And the ergodic rate for nearest F-AP mode under the conditions in (5) can be given as

$$\begin{aligned}
R_f &= p_F \mathbb{E}[\ln(1 + \gamma_f) | \gamma_f \geq T_f] \\
&\approx \int_{\ln(T_f)}^\infty p_F P_F(e^\theta, \alpha_f, p_c^F) d\theta + p_F \ln(T_f) P_F(T_f, \alpha_f, p_c^F). \tag{17}
\end{aligned}$$

Special Case: Path loss exponent for F-AP to user link is 4 ($\alpha_f = 4$), and SIR threshold $T_f > 1$

A closed-form approximate expression can be derived in this special case, and we give the ergodic rate as Lemma 1.

Lemma 1: The ergodic rate for nearest F-AP mode with $\alpha_f = 4$ and $T_f > 1$ can be expressed as

$$\begin{aligned}
R_f^{\alpha_f=4} &= p_F \mathbb{E}[\ln(1 + \gamma_f) | \gamma_f \geq T_f] \\
&\approx \frac{4p_F}{\pi \sqrt{T_f} \left(1 + \frac{\lambda_{du}}{p_c^F \lambda_f} \sqrt{\frac{P_d}{P_f}}\right)} + \frac{2p_F \ln(T_f)}{\pi \sqrt{T_f} \left(1 + \frac{\lambda_{du}}{p_c^F \lambda_f} \sqrt{\frac{P_d}{P_f}}\right)} \\
&= \frac{2p_F (2 + \ln(T_f))}{\pi \sqrt{T_f} \left(1 + \frac{\lambda_{du}}{p_c^F \lambda_f} \sqrt{\frac{P_d}{P_f}}\right)}. \tag{18}
\end{aligned}$$

Proof: See Appendix B. ■

C. Local distributed coordination mode

Lastly, we discuss the local distributed coordination mode that the desired U associates to multiple F-APs near to it in a user-centric cluster with a distance threshold L_c . This mode is triggered if U don't meet the conditions of both the first two modes, i.e.,

$$\begin{aligned}
p_C &= (1 - p_D P_D(T_d, \alpha_f, \alpha_d, \|X_d\|)) \\
&\cdot (1 - P_F(T_f, \alpha_f, p_c^F)) \\
&= p_f (1 - P_F(T_f, \alpha_f, p_c^F)). \tag{19}
\end{aligned}$$

To extend to access the arbitrary F-APs, the main problem here is the exact PDF expression of $\sum_{v \in \Psi_C} P_f h_v \|X_v\|^{-\alpha_f}$ is very difficult to obtain, so we tried to get around this problem by following the Lemma 1 in [14].

For any $A > 0$

$$\mathbb{E}[\ln(1 + A)] = \int_0^\infty \frac{1}{z} (1 - e^{-Az}) e^{-z} dz \tag{20}$$

Therefore, with (20), the ergodic rate expression can be written as (21) on the top of next page, where (a) follows set $s = z \cdot (I_{f,cu} + I_{d,fu})$, (b) follows $c \in \Psi_C \cup \{\Phi_f / \Psi_C\} = \Phi_f$.

D. Adaptation user access mode selection mechanism

In addition, based on communication distance, nodes location, SIR QoS requirements and caching capabilities, an adaptation mode selection mechanism is presented in this subsection to take full advantages of these three modes.

Algorithm 1 Adaptation User Access Mode Selection mechanism

- 1: **Initialize** $\Psi_D = \emptyset, \Psi_F = \emptyset, \Psi_C = \emptyset$.
 - 2: **Step 1** Check the cache content of another D2D user near by the desired user U with a radius threshold L_d , $B(U, L_d) \cap \Phi_{du} = \{X_1, X_2, \dots, X_D\}$.
 - 3: **for** $i = 1, 2, \dots, D$ **do**.
 - 4: **if** $V \in C_d^i$
 - 5: Calculate the SIR γ_d^i from (7).
 - 6: **if** $\gamma_d^i \geq T_d$.
 - 7: $X_i \in \Psi_D$ User select **D2D mode** with X_i . **break**
 - 8: **end if**
 - 9: **end if**
 - 10: **end for**
 - 11: **Step 2** Find the nearest F-AP of the desired user U in $\Phi_f = \{X_1, X_2, \dots, X_F\}$.
 - 12: **Set** $\|X_f\| = \|X_1\|$.
 - 13: **for** $j = 2, 3, \dots, F$ **do**.
 - 14: **if** $\|X_j\| < \|X_f\|$.
 - 15: Nearest node $\|X_f\| = \|X_j\|$.
 - 16: **end if**
 - 17: **end for**
 - 18: **if** $V \in C_f^j$
 - 19: Calculate the SIR γ_f with $\|X_f\|$ from (8).
 - 20: **if** $\gamma_f \geq T_f$.
 - 21: $X_f \in \Psi_F$ User select **1 FAP mode** with X_f .
 - 22: **else**
 - 23: go to **Step 3**
 - 24: **end if**
 - 25: **end if**
 - 26: **Step 3** User select **local distributed coordination mode** with $\Psi_F = B(U, L_f) \cap \Phi_f = \{X_1, X_2, \dots, X_F\}$.
-

IV. NUMERICAL RESULTS

In this section, the accuracy of the above ergodic rate expressions and the impact of λ , C and T on rate performance are evaluated by using Matlab with Monte Carlo simulation method. The simulation parameters are listed as follows in Table I.

Fig. 1 shows the ergodic rate achieved by the D2D mode with the varying distance between D2D pairs in the cases of different SIR QoS thresholds T_d . The analytical results closely match with the corresponding simulation results, which validates our analysis in Section III. It can be observed that the ergodic rate of D2D mode decreases as the distance between D2D pair increases. Similarly, the larger T_d suggests that the D2D user is more strict in the quality of SIR, which leads to

$$\begin{aligned}
R_c &= p_C \mathbb{E} \left[\ln \left(1 + \frac{\sum_{c \in \Psi_C} P_f h_c \|X_c\|^{-\alpha_f}}{I_{f,cu} + I_{d,fu}} \right) \right] = p_C \mathbb{E} \left[\int_0^\infty \frac{e^{-z}}{z} \left(1 - \exp \left(-\frac{z \sum_{c \in \Psi_C} P_f h_c \|X_c\|^{-\alpha_f}}{I_{f,cu} + I_{d,fu}} \right) \right) dz \right] \\
&\stackrel{(a)}{=} p_C \mathbb{E}_{\Phi, h, g} \left[\int_0^\infty \frac{1}{s} \exp(-s(I_{f,cu} + I_{d,fu})) \left[1 - \exp \left(-s \sum_{c \in \Psi_C} P_f h_c \|X_c\|^{-\alpha_f} \right) \right] ds \right] \\
&\stackrel{(b)}{=} p_C \int_0^\infty \frac{1}{s} \left\{ \mathbb{E}_{\Phi, h, g} \left[\exp(-s(I_{f,cu} + I_{d,fu})) - \exp \left(-s \left(I_{d,fu} + \sum_{c \in \Phi_f} P_f h_c \|X_c\|^{-\alpha_f} \right) \right) \right] \right\} ds \\
&= p_C \int_0^\infty \frac{1}{s} \left\{ L_{I_{f,cu}}(s) L_{I_{d,fu}}(s) - L_{I_{d,fu}}(s) L_{\sum_{c \in \Phi_f} P_f h_c \|X_c\|^{-\alpha_f}}(s) \right\} ds \\
&= p_C \int_0^\infty \frac{1}{s} \exp \left(-\pi \lambda_{du} C(\alpha_f) (P_d s)^{\frac{2}{\alpha_f}} \right) \left[\exp \left(-2\pi p_C^F \lambda_f \int_R^\infty \frac{P_f s v}{v^{\alpha_f} + P_f s} dv \right) - \exp \left(-\pi p_C^F \lambda_f C(\alpha_f) (P_f s)^{\frac{2}{\alpha_f}} \right) \right] ds,
\end{aligned} \tag{21}$$

TABLE I
SIMULATION PARAMETERS

Parameters	Value
Number of video content N	1000
Caching size of D2D user C_d	50
Caching size of F-AP C_f	200 ~ 800
Intensity of D2D users $p\lambda_u$	1×10^{-3}
Intensity of F-AP nodes λ_f	$1 \times 10^{-4} \sim 1 \times 10^{-3}$
Path loss exponent α	4 [15]
D2D user Zipf exponent σ_d	0.8
F-AP Zipf exponent σ_f	1
Transmit power of D2D user P_d	3dBm [16]
Transmit power of F-AP P_f	23dBm
D2D distance threshold L_c	16m

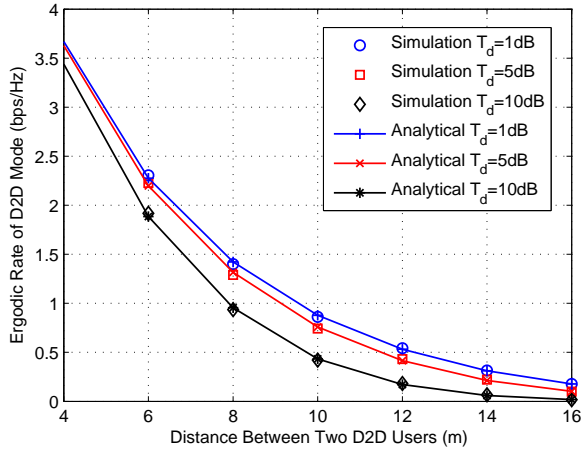


Fig. 1. Ergodic rate of D2D mode with different SIR thresholds versus distance between two D2D users.

less user select D2D mode, and thus D2D mode ergodic rate decreases.

Ergodic rate of nearest F-AP mode with different SIR thresholds versus intensity of F-AP nodes λ_f is shown in Fig. 2. As we see from Fig. 2, the ergodic rate of nearest F-AP mode grows as the nodes intensity λ_f increases until it reaches its upper bound. It is worth noting that the ergodic rate of nearest F-AP mode seems lower than the D2D mode, this is because the users which have good SIR are more inclined to selected D2D mode. On the other hand, when the SIR threshold increases, the ergodic rate of nearest F-AP mode follows similar trend as D2D mode.

In Fig. 3, we compare the ergodic rate of local distributed

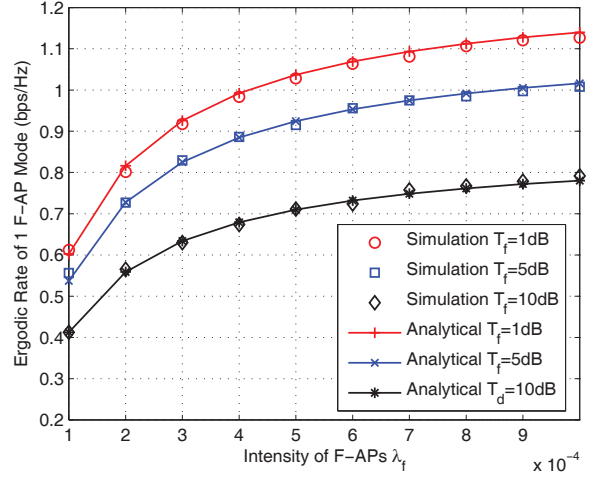


Fig. 2. Ergodic rate of nearest F-AP mode with different SIR thresholds versus intensity of F-AP nodes λ_f .

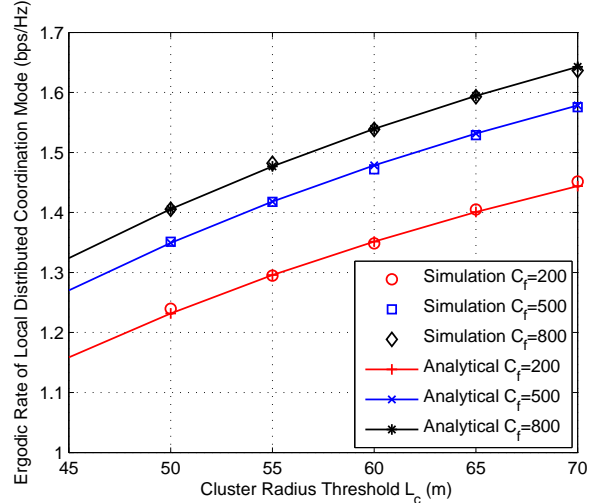


Fig. 3. Ergodic rate of local distributed coordination mode with different F-AP cache size versus cluster radius threshold L_c , $\lambda_f = 2 \times 10^{-4}$.

coordination mode with different F-AP cache sizes versus cluster radius threshold L_c . Since the number of F-APs in the cluster increases with L_c , it means more F-APs are serving the desired user with the increase of signal and the decline of interference. And it leads to the enlargement of cluster SIR and results in the improvement of ergodic rate of local distributed coordination mode. Similarly, the larger cache size of F-AP C_f suggests that there are more opportunities for the desired user to get the video content it needs, which leads to a higher

ergodic rate.

V. CONCLUSION

In this paper, the expressions of coverage probability and ergodic rates in downlink F-RAN system under three user access modes have been derived. The impact of the cache size, SIR threshold cluster radius and nodes intensity on the coverage probability and ergodic rate are researched. Moreover, an adaptation user access mode selection mechanism is proposed to improve F-RAN system performances.

VI. ACKNOWLEDGEMENT

This work is supported in part by the National Natural Science Foundation of China (Grant No. 61222103 and 61361166005), the National Basic Research Program of China (973 Program) (Grant No. 2013CB336600).

APPENDIX

A. Proof of R_d

For a positive continuous random variable A , we can use the following formula for computing its expectation

$$\begin{aligned} \mathbb{E}[A|A \geq W] &= \int_W^\infty t f_A(t) dt = \int_W^\infty \int_0^t f_A(t) da dt \\ &= \int_0^\infty \int_W^\infty f_A(t) dt da + \int_W^\infty \int_a^\infty f_A(t) dt da \\ &= \int_0^W \Pr(A \geq W) da + \int_W^\infty \Pr(A \geq a) da \\ &= W \Pr(A \geq W) + \underbrace{\int_W^\infty \Pr(A \geq a) da}_S \end{aligned} \quad (22)$$

Next, we focus on the second term of (22), after changing variables with $W = \ln(T_d)$, $A = \ln(1 + \gamma_f)$ and $a = \theta$ the expression of this term can be given as

$$\begin{aligned} S &= \int_{\ln(T_d)}^\infty \Pr\left(\frac{P_d h_d \|X_d\|^{-\alpha_d}}{I_{d,du} + I_{f,du}} > e^{\theta_d} - 1\right) d\theta_d \\ &\approx \int_{\ln(T_d)}^\infty L_{I_{d,du}}\left(\frac{e^{\theta_d} \|X_d\|^{\alpha_d}}{P_d}\right) L_{I_{f,du}}\left(\frac{e^{\theta_d} \|X_d\|^{\alpha_d}}{P_d}\right) d\theta_d \\ &= \int_{\ln(T_d)}^\infty \exp\left(-\pi \|X_d\|^{\frac{2\alpha_d}{\alpha_f}} \beta C(\alpha_f) e^{\frac{2\theta_d}{\alpha_f}}\right) d\theta_d \\ &= -\frac{\alpha_f}{2} \text{Ei}\left(-T_d^{\frac{2}{\alpha_f}} \pi \|X_d\|^{\frac{2\alpha_d}{\alpha_f}} \beta C(\alpha_f)\right), \end{aligned} \quad (23)$$

where $\beta = \left(\lambda_{du} + (P_f/P_d)^{2/\alpha_f} \lambda_f\right)$, and the proof is finished.

B. Proof of lemma 1

we first drive the coverage probability of nearest F-AP mode with $\alpha_f = 4$ and $T_f > 1$, which can be denoted as

$$\begin{aligned} P_F^{\alpha_f=4}(T_f, p_c^F) &= \frac{1}{1 + \rho(T_f, 4) + \frac{\lambda_{du}}{p_c^F \lambda_f} C(4) \sqrt{\frac{P_d T_f}{P_f}}} \\ &= \frac{1}{1 + \sqrt{T_f} \int_{1/\sqrt{T_f}}^\infty \frac{1}{1+v^2} dv + \frac{\pi \lambda_{du}}{2 p_c^F \lambda_f} \sqrt{\frac{P_d T_f}{P_f}}} \\ &= \frac{1}{1 + \sqrt{T_f} \left[\frac{\pi}{2} - \arctan(1/\sqrt{T_f})\right] + \frac{\pi \lambda_{du}}{2 p_c^F \lambda_f} \sqrt{\frac{P_d T_f}{P_f}}} \\ &\stackrel{(a)}{\approx} \frac{1}{1 + \sqrt{T_f} \left[\frac{\pi}{2} - (1/\sqrt{T_f})\right] + \frac{\pi \lambda_{du}}{2 p_c^F \lambda_f} \sqrt{\frac{P_d T_f}{P_f}}} \\ &= \frac{2}{\pi \sqrt{T_f} \left(1 + \frac{\lambda_{du}}{p_c^F \lambda_f} \sqrt{\frac{P_d}{P_f}}\right)}, \end{aligned} \quad (24)$$

where (a) follows the property of the inverse trigonometric functions that $\arctan(A) \approx A$ if A is smaller than 1, i.e., $T_f \geq 1$.

Then, substituting (24) into (22) with $W = \ln(T_f)$ and we obtain the result.

REFERENCES

- [1] M. Peng, Y. Li, Z. Zhao, and C. Wang, "System architecture and key technologies for 5G heterogeneous cloud radio access networks," *IEEE Network*, vol. 29, no. 2, pp. 6-14, Mar. 2015.
- [2] M. Peng, C. Wang, V. Lau and H. V. Poor, "Fronthaul-constrained cloud radio access networks: Insights and challenges," *IEEE Wireless Commun.*, vol. 22, no. 2, pp. 152-160, April 2015.
- [3] M. Peng, Y. Li, J. Jiang, J. Li, and C. Wang, "Heterogeneous cloud radio access networks: A new perspective for enhancing spectral and energy efficiencies," *IEEE Wireless Commun.*, vol. 21, no. 6, pp. 126-135, Dec. 2014.
- [4] M. Peng, S. Yan, K. Zhang, and C. Wang, "Fog computing based radio access networks: Issues and challenges", to appear in *IEEE Networks*, [Online]. Available: <http://arxiv.org/abs/1506.04233>
- [5] Cisco technology radar trends: Fog computing. [Online]. Available: <http://www.cisco.com/web/solutions/trends/tech-radar/fogcomputing.html>
- [6] M. Peng, S. Yan, H. V. Poor, "Ergodic capacity analysis of remote radio head associations in cloud radio access networks", *IEEE Wireless Commun. Letters*, vol. 3, no. 4, pp. 365-368, Aug. 2014.
- [7] A. Liu and V. Lau, "Joint power and antenna selection optimization in large cloud radio access networks", *IEEE Trans. Signal Processing*, vol. 62, no. 5, pp. 1319-1328, Mar. 2014.
- [8] D. Feng, L. Lu, G.Y. Li, et al., "Device-to-device communications underlying cellular networks", *IEEE Trans. Commun.*, vol. 61, no. 8, pp. 3541-3551, Jul. 2013.
- [9] H. Elsawy, E. Hossain, M.S. Alouini, "Analytical modeling of mode selection and power control for underlay D2D communication in cellular networks", *IEEE Trans. Commun.*, vol. 612, no. 11, pp. 4147-4161, Oct. 2014.
- [10] Y. Li, D. Jin, J. Yuan, Z. Han, "Coalitional games for resource allocation in the device-to-device uplink underlying cellular networks", *IEEE Trans. Wireless Commun.*, vol. 13, no. 7, pp. 3965-3977, May 2014.
- [11] L. Breslau, P. Cao, L. Fan et al., "Web caching and Zipf-like distributions: Evidence and implications", *Proc. IEEE INFOCOM 1999*.
- [12] J. Andrews, F. Baccelli, and R. Ganti, "A tractable approach to coverage and rate in cellular networks," *IEEE Trans. Commun.*, vol. 59, no. 11, pp. 3122-3134, Nov. 2011.
- [13] F. Baccelli, B. Blaszczyszyn, and P. Uhlethaler, "Stochastic analysis of spatial and opportunistic ALOHA," *IEEE J. Sel. Areas Commun.*, vol. 27, no. 7, pp. 1105-1119, Sep. 2009.
- [14] K. Hamdi, "Capacity of MRC on correlated rician fading channels", *IEEE Trans. Commun.*, vol. 56, no. 5, pp. 708-711, May 2008.
- [15] W. Cheung, T. Quek, and M. Kountouris, "Throughput optimization, spectrum allocation, and access control in two-tier femtocell networks," *IEEE J. Sel. Areas Commun.*, vol. 30, no. 3, pp. 561-574, Apr. 2012.
- [16] M. Peng, Y. Li, T. Quek, and C. Wang, "Device-to-device underlaid cellular networks under Rician fading channels", *IEEE Trans. Wireless Commun.*, vol. 13, no. 8, pp. 4247-4259, Aug. 2014.